Synthesis, structure, Hirshfeld surface analysis and computational studies of 2-amino-5-nitropyridine-2,4-dinitrophenol cocrystal

Shanmugam Sivaraman
Annamalai University
Chellakarungu Balakrishnan
Annamalai University
Palusamy Suppuraj
Annamalai University
Subbiah Meenakshisundaram (ssmanchem@gmail.com)
Annamalai University

Research Article

Keywords: 2-amino-5-nitropyridine cocrystal, supramolecular assembly, thermal stability, hyperpolarizability

Posted Date: September 22nd, 2022

DOI: https://doi.org/10.21203/rs.3.rs-2036200/v1

Abstract

Crystal structure of 2-amino-5-nitropyridine-2,4-dinitrophenol (ANDP) grown by slow evaporation solution growth method was elucidated by single crystal X-ray diffraction analysis and it belongs to monoclinic system with centrosymmetric space group P21/n. The crystallinity and homogeneity of the material was confirmed by powder X-ray diffraction which agrees well with the simulated pattern with varied intensities. The functional groups present in the molecule are identified by FT-IR analysis and the band gap energy was estimated using diffuse reflectance data by the application of Kubelka-Munk algorithm. The thermal stability of the compound was investigated by carrying out TG-DTA analysis. Theoretical calculations were performed using density functional theory method to derive the dipole moment and hyperpolarizability. High value of first-order molecular hyperpolarizability (β) suggests that it is a potential microlevel NLO candidate.

Introduction

Supramolecular crystals have attractive molecular architectures for useful applications. Understanding intermolecular interactions can provide valuable information useful in the design of new crystals [1]. One or more delocalized bonds that, when exposed to electromagnetic fields, produce a high induced dipole moment, often in the form of a ring structure like benzene with donors and acceptors substituted at the *para* positions [2]. Modern research has shown that organic materials offer superior nonlinear optical (NLO) characteristics [3], optoelectronic materials [4] and data storage devices [5]. Phenol derivatives are interesting crystals, as the existence of the phenolic (–OH) group favors the formation of salts with several organic bases [6-8]. Additionally, by interactions with diverse organic compounds *via* π-bonding and hydrogen bonding, it forms cocrystals [9-11]. To some extent, molecular designs have been successful in improving charge transfer and first-order molecular hyperpolarizability (β). Intermolecular hydrogen bonding leads to the close packing of molecules within the crystal medium that is necessary for efficient nonlinear optical properties, along with van der Waals, molecular dipolar and quadruple forces for energy minimization [12]. Many organic compounds with photosensitivity and thermal stability have recently been developed that are helpful in creating different crystalline electro-optical systems [13-14].

In the current study, we describe a unique supramolecular cocrystal structure that was described utilizing Hirshfeld surface, single-crystal and powder X-ray diffraction, UV diffuse reflectance and photoluminescence spectroscopy and thermal analysis. The experimental results were also supported by computational investigations.

Experimental

Synthesis

2-Amino-5-nitropyridine-2,4-dinitrophenol (ANDP) cocrystal was synthesized by mixing equimolar quantities of 2-ammino-5-nitropyridine (ANP) and 2,4-dinitrophenol (DNP) in ethanol. The mixture was stirred at room temperature for 4 h (Scheme 1). The product was purified by recrystallization using ethanol as solvent. The transparent crystals were harvested in 7-10 d.

Characterization techniques

A Bruker D8 QUEST single-crystal X-ray diffractometer (MoKα radiation (λ = 0.71073 Å) was used for single-crystal XRD studies. The structure is refined for the computer programs APEX3, APEX3/SAINT, SAINT V8.38A, SHELXT 2014/5, SHELXL-2018/3 and shelXle. A Philips Xpert pro triple-axis X-ray diffractometer (CuKα radiation in the 2θ range of 10–50º) was used for powder X-ray diffraction analysis. A Shimadzu IR Affinity-1 FT-IR spectrophotometer was used for recorded FT-IR spectrum. The ultraviolet diffuse reflectance spectrum (UV–DRS) was recorded by Shimadzu UV-2600 spectrophotometer. Photoluminescence spectrum was recorded by HJY:Fluorolg F3-111 fluorescence spectrometer. Hirshfeld surfaces and fingerprint plots were generated by CrystalExplorer 3.1 program [15]. All theoretical calculations were performed using the GAUSSIAN09W program using density functional theory (DFT) with B3LYP method 6-311G(d,p) as the basis set [16].

Results And Discussion

XRD analysis

The as-grown crystal was finely powdered and subjected to powder XRD analysis. The bulk phase purity and homogeneity of ANDP were confirmed by matching experimental diffractograms with calculated patterns from the single crystal XRD data. No significant variations are observed in peak positions of experimental and simulated XRD patterns (Fig. 1).

The crystal structure was determined by single-crystal X-ray diffraction and the crystallographic data are shown in Table 1. Selected bond lengths, angles and torsion angles are listed in Table S1. Cocrystal ANDP grown from ethanol crystallizes in the centrosymmetric monoclinic system with space group $P2_1/n$ and Z = 4. A displacement ellipsoid plot and molecular packing diagram of ANDP are shown in Fig. 2. ANP and DNP molecules alternate in zig-zag chains and hydrogen atom was not transferred from the DNP to ANP. Supramolecularly assembled by N-H•••O, N-H•••N, O-H•••O, O-H•••N and C-H•••O hydrogen bonds. An infinite column-like structure is formed *via* π•••π staking interactions between ANP and DNP as shown in Fig. 3(a) and it matches to the structural arrangement of paracetamol with picric acid [11]. The centroid-centroid contact distance range is 3.609 to 3.896 Å with angle ranging from 19.13 to 22.59°. Plane to plane distance ranges from 3.427 to 3.596 Å. Fig. 3(b) displays the N-H•••O and N-H•••N intermolecular interactions. The intramolecular interaction (O(5)-H(5A)•••O(6)) is the shortest hydrogen bond observed in DNP molecule with a distance of 2.6047(18) Å (Fig. 4(a)). Fig. 4(b) shows the weak C-H•••O interactions and they are listed in Table 2.

FT-IR spectroscopy

The vibrational spectrum exhibits the characteristic bands of 2-amino-5-nitropyridine and 2,4-dinitrophenol. The band observed at 3295 cm^{-1} corresponds to the symmetric stretching vibration of phenolic O-H group of DNP molecule. The absorption band around 3457 cm^{-1} is due to N-H stretching frequency of the amino group. The N-H bending vibration is observed at 1627 cm^{-1}. The bands appeared at around 1568 and 1325 cm^{-1} are due to the asymmetric and symmetric stretching vibrations of -NO_2 group respectively. The aromatic
C-H stretching frequency appears around 3093 cm^{-1}. The aromatic ring C=C stretching vibrations are assigned to peak at 1595 cm^{-1}. The IR spectra vibrational frequencies of
2-amino-5-nitropyridine (SDBS No: 4210), 2,4-dinitrophenol (SDBS No: 2390) and ANDP are shown in Fig. S1.

Optical studies

The optical reflectance spectrum of ANDP (Fig. 5) reveals high transmittance and cut-off wavelength is ~434 nm. Band gap is estimated using Tauc plot, $[F(R)h\ ]^2$ *versus* h and the estimated direct band gap energy of ANDP is 2.79 eV. The cocrystal exhibits fluorescent emission at λ_{max} 649 nm (~1.91 eV) under the excitation at 434 nm in the solid-state at room temperature (Fig. 6).

Thermal analysis

The thermogravimetric analysis (TGA) and differential thermal analysis (DTA) were recorded over a range of 28-600°C under nitrogen atmosphere at a heating rate of 20 K min^{-1}. Fig. 7 shows the TG-DTA curve of ANDP. In TGA curve the major weight loss is 82.5% observed over the temperature range from 182 to 312°C. In DTA trace, the endothermic peak at 112°C corresponds to the melting point of ANDP.

Hirshfeld surface analysis

Fig. 8 shows surfaces that have been mapped over dnorm, d_i, d_e, shape index and curvedness. The surfaces are shown as transparent to allow visualization of the molecule around which they were calculated. Hydrogen bonding contacts are revealed by circular depressions (deep red) observable on the Hirshfeld surface, and the other visible spots in
Fig. 8 are due to O•••H;H•••O (42.1%) interactions.

The combination of d_e and d_i in the form of a two-dimensional fingerprint plot provides a summary of intermolecular contacts in the crystal (Fig. 9). The O•••H;H•••O (42.1%) interactions are represented by a spike at the inner bottom of the plot in the inner top left region. The H•••H (12.2%) interactions are observed at the center of the fingerprint plot. In the top right corner, O•••O (9.3%) interactions are shown. Strong interactions occupy more space and weak interactions occupy less space in the fingerprint plot. Quantification of all intra- and intermolecular interactions are displayed as a pie chart Fig. S2.

First-order molecular hyperpolarizability

The NLO responses in organic compounds originate from π-electron excitation of individual molecules. The molecular level NLO response is confirmed by computational studies. Calculated polarizability (α), first-order molecular hyperpolarizability (β) and dipole moment (μ) of the specimen are, 27.6680 × 10^{-24} esu, 1.6596 × 10^{-30} esu (∼9 times of urea) and 5.8347 D, respectively (Table 3). As shown in the table β_{xxy} tensor mainly contributes to the nonzero β value. Generally, high β_{tot} value is ascribed to conjugation, molecular symmetry, hyperconjugation, substitution, aromaticity and charge transfer [17]. High value of β suggests that the title compound has a good microlevel NLO response.

Frontier molecular orbital (FMO) analysis

Fig. 10 displays the highest occupied molecular orbital (HOMO) and lowest unoccupied molecular orbital (LUMO), calculated using B3LYP/ 6-311G(d,p) as basis set and 2D images of orbitals computed in gaseous state. The red color indicates the positive value and the green color indicates the negative value of wave function. The HOMO is localized on the ANP molecule whereas LUMO localized on the DNP molecule. Both HOMO and LUMO are mostly π-antibonding type orbitals. Orbital is plotted at an isosurface value 0.02 a.u. The calculated energy values are, -7.0352 eV (HOMO), -4.0159 eV (LUMO) and 3.02 eV (energy gap). $\Delta E_{HOMO\text{-}LUMO}$ explains the eventual charge transfer interactions with in the molecule. Small frontier orbital gap facilitates polarizability and hence the title cocrystal is a promising candidate for NLO applications. The band gap derived from FMOs is higher than the experimental value. The experimental band gap is 2.79 eV, whereas the theoretical band gap is 3.02 eV. Variation in justified since the theoretical studies are for the gas phase, whereas the experiments are done in the condensed phase [18].

Mulliken population analysis

Mulliken charges arise from the Mulliken population analysis and provide a means of estimating partial atomic charges from calculations carried out by the methods of computational chemistry. Mulliken atomic charge distribution is displayed in
Fig. S3. All the oxygen, carbon (C2, C6, C8 and C24) and nitrogen (N26 and N27) are negative charges behaving as electron donors, whereas remaining carbons (C1, C4, C5, C18, C19, C21 and C22), all the hydrogen atoms and nitrogen (N10, N11 and N28) are acceptors revealing positive charge (Table S2).

Molecular electrostatic potential (MEP)

The MEP plot of electrostatic potential mapped on the constant electron density surface displaying electrostatic potential distribution is shown in Fig. S4. The most negative electrostatic potential surfaces are represented as the red colour that are expected to be sites of protonation and nucleophilic attack whereas most positive electrostatic potential specifies the blue colour and the green denotes regions of zero potential. The colour code of this map is in the range between −5.729e^{-2} to +5.729e^{-2}.

Conclusions

Single crystals 2-amino-5-nitropyridine-2,4-dinitrophenol were successfully grown by the slow evaporation solution growth method at room temperature. The grown crystals have been subjected to various characterization studies. The crystallographic data indicate that the title compound crystallizes in the monoclinic system with centrosymmetric space group $P2_1/n$. Minimum absorbance in the visible region coupled with high first-order molecular hyperpolarizability (β) in comparison with standard urea reveals good microlevel NLO response of the title compound. Prominent O•••H/H•••O interactions contribute to microlevel nonlinearity. Substitution of suitable donor-acceptor groups in the aromatic ring could make it SHG-active. Molecular electrostatic potential surfaces visualize the relative polarity and population analysis suggest the possibility of inter- and intramolecular charge transfer interactions responsible for observed nonlinearity.

Abbreviations

ANDP	2-Amino-5-nitropyridine-2,4-dinitrophenol
ANP	2-Ammino-5-nitropyridine
DNP	2,4-Dinitrophenol
FT-IR	Fourier transform infrared spectroscopy
TG-DTA	Thermogravimetric and differential thermal analysis
NLO	Nonlinear optical
SHG	Second harmonic generation
MEP	Molecular electrostatic potential
DFT	Density functional theory
FMO	Frontier molecular orbitals
HOMO	Highest occupied molecular orbital
LUMO	Lowest unoccupied molecular orbital
UV-Vis DRS	Ultraviolet visible near-infrared diffuse reflectance spectroscopy
XRD	X-ray diffraction
CCDC	Cambridge Crystallographic Data Centre

Declarations

Supplementary materials

CCDC **1871547** contain the supplementary crystallographic data for this paper. These data can be obtained free of charge from The Cambridge Crystallographic Data Centre via www. ccdc.cam.ac.uk/data request/cif.

Funding

The authors thank the Council of Scientific and Industrial Research, New Delhi, for financial support through research grant No. 21 (1024)/16/EMR-II. SS and CB are grateful to the CSIR Emeritus Scientist Scheme for the award of the SRF/RA-ship.

Conflicts of interest/Competing interests

Conflict of interest the authors declare no competing interests.

Availability of data and material

Not applicable

Author contribution

S S: data curation, investigation, visualization, validation, writing, original draft. C B: data curation, investigation, visualization, validation. P S: investigation. SP M: review, editing, and supervision. The final version of the manuscript submitted was approved by all the authors.

References

1. Wang, K., Duan, D., Wang, R., Lin, A., Cui, Q., Liu, B., Cui, T., Zou, B., Zhang, X., Hu, J., Zou, G. & Mao, H. (2009). Langmuir, 25, 4787–4791.
2. Ng, S. L., Patil, P. S., Razak, I. A., Fun, H.-K. & Dharmaprakash, S. M. (2006). Acta Cryst. E62, o1228–o1230.
3. S. Basu, Ind. Eng. Chem. Prod. Res. Dev. 23, 183–186 (1984)
4. C. Liu, A.J. Bard, Acc. Chem. Res. 32, 235–245 (1999)
5. O. Ostroverkhova, Chem. Rev. 116, 13279–13412 (2016)
6. Z.M. Jin, Y.J. Pan, D.J. Xu, Y.Z. Xu, Acta Crystallogr. C 56, e69–e70 (2000)
7. C. Indumathi, T.S. Girisun, K. Anitha, S.A.C. Raj, Opt.Mater. 60, 214–220 (2016)
8. M. Manonmani, C. Balakrishnan, S.P. Meenakshisundaram, R.M. Sockalingam, Mater. Today 15, 645–653 (2019)
9. P. Karuppasamy, T. Kamalesh, K. Anitha, S.A. Kalam, M.S. Pandian, P. Ramasamy, S. Verma, S.V. Rao, Opt. Mater. 84, 475–489 (2018)

10. R. Moreno-Fuquen, F. Cano, M. Martinez-Ripoll, A. Montano, J. Zukerman-Schpector, Acta Crystallogr. E 57, o712–o714 (2001)
11. M. Manonmani, C. Balakrishnan, S.R. Ahamed, G. Vinitha, S.P. Meenakshisundaram, R.M. Sockalingam, J. Mol. Struct.1190, 1–10 (2019)
12. Reshak, A. H., Alahmed, Z. A. & Azam, S. (2014). Int. J. Electrochem. Sci. 9, 975–989.
13. Williams, D. (1983). Nonlinear Optical Properties of Organic and Polymeric Materials.Washington, DC: American Chemical Society.
14. Phrutivorapongkul, A., Lipipun, V., Ruangrrungsi, N., Kiritikara, K.,Nishikawa, K., Maruyama, S., Watanebe, T. & Ishikawa, T. (2003).Chem. Pharm. Bull. 51, 187–190.
15. Wolff, S. K., Grimwood, D. J., McKinnon, J. J., Turner, M. J., Jayatilaka, D. & Spackman, M. A. (2012). CrystalExplorer (Version 3.1). University of Western Australia.
16. Frisch, M. J., et al. (2009). GAUSSIAN09, Revision C.01. Gaussian, Inc., Wallingford, CT, USA.
17. J. Zyss and J. L. Oudar*, Phy. Rew A*, **26** (1982)2028-2048.
18. Jauhar, R. M., & Murugakoothan, P. (2017). *AIP Conf. Proc,* 1832, 100005-1.

Tables

Table 1 Crystal data and structure refinement

CCDC No	1871547	
Empirical formula	$C_{11}H_9N_5O_7$	
Formula weight	323.23	
Temperature	296(2) K	
Wavelength	0.71073 Å	
Crystal system	Monoclinic	
Space group	$P2_1/n$	
Unit cell dimensions	a = 11.2573(8) Å	α = 90°
	b = 9.1259(5) Å	β = 107.758(2)°
	c = 13.4593(9) Å	γ = 90°
Volume	1316.83(15) $Å^3$	
Z	4	
Density (calculated)	1.630 Mg/m^3	
Absorption coefficient	0.139 mm^{-1}	
F(000)	664	
Crystal size	0.200 x 0.150 x 0.150 mm^3	
Theta range for data collection	3.601 to 24.990°	
Index ranges	-13<=h<=13, -10<=k<=10, -16<=l<=16	
Reflections collected	17300	
Independent reflections	2308 [R(int) = 0.0582]	
Completeness to theta = 24.990°	99.6 %	
Absorption correction	Semi-empirical from equivalents	
Max. and min. transmission	0.7462 and 0.4096	
Refinement method	Full-matrix least-squares on F^2	
Data / restraints / parameters	2308 / 3 / 216	
Goodness-of-fit on F2	1.072	
Final R indices [I>2sigma(I)]	R1 = 0.0426, wR2 = 0.1088	
R indices (all data)	R1 = 0.0569, wR2 = 0.1206	

Extinction coefficient	n/a
Largest diff. peak and hole	0.217 and -0.205 e.Å^{-3}

Table 2 Hydrogen bonds [Å and °]

D-H•••A	d(D-H)	d(H•••A)	d(D•••A)	<(D-H•••A)
C(5)-H(5)•••O(1)#1	0.93	2.54	3.4485(19)	164.9
C(6)-H(6)•••O(5)#2	0.93	2.62	3.4086(19)	143.1
C(8)-H(8)•••O(6)#3	0.93	2.51	3.306(2)	144.3
C(10)-H(10)•••O(2)	0.93	2.47	3.3407(19)	156.8
C(11)-H(11)•••O(3)#4	0.93	2.59	3.450(2)	153.9
O(5)-H(5A)•••N(2)	0.82	2.51	2.9280(18)	113.0
O(5)-H(5A)•••O(1)#5	0.82	2.45	2.9597(17)	121.6
O(5)-H(5A)•••O(4)	0.82	1.91	2.6047(18)	141.3
N(3)-H(3B)•••O(6)#4	0.815(14)	2.577(19)	3.018(2)	115.4(15)
N(3)-H(3A)•••N(4)#6	0.849(15)	2.259(16)	3.099(3)	170(2)

Symmetry transformations used to generate equivalent atoms: #1 -x+1/2,y-1/2,-z+3/2 #2 -x+1/2,y+1/2,-z+3/2 #3 -x+1,-y+1,-z #4 x,y+1,z #5 x,y-1,z #6 -x+1,-y+2,-z

Table 3 The calculated β components (a.u.), β_{tot} value (in esu), α components (a.u.), α_{tot} value (in esu) and dipole moment (in D)

First-order molecular hyperpolarizability	
β_{xxx}	84.9264
β_{xxy}	135.6566
β_{xyy}	25.4835
β_{yyy}	18.0133
β_{xxz}	75.3246
β_{xyz}	21.4366
β_{yyz}	-0.9604
β_{xzz}	-10.5418
β_{yzz}	-10.5182
β_{zzz}	5.8725
β_{total} (esu)	**1.6596×10^{-30}**
Polarizability	
α_{xx}	-117.3678
α_{xy}	-3.3076
α_{yy}	-145.6472
α_{xz}	6.5147
α_{yz}	0.8215
α_{zz}	-129.6220
α_{tot} (esu)	**27.6680×10^{-24}**
Dipole moment (D)	
μ_x	1.1062
μ_y	5.6296
μ_z	1.0620
μ	**5.8347**

Table 4 Mulliken atomic charges

Atoms	Charges (e)	Atoms	Charges (e)	Atoms	Charges (e)	Atoms	Charges (e)
C1	0.1138	H9	0.1583	H17	0.2665	H25	0.1181
C2	-0.0011	N10	0.1777	C18	0.2878	N26	-0.4302
H3	0.2097	N11	0.1214	C19	0.1302	N27	-0.3478
C4	0.1525	O12	-0.2616	H20	0.1580	N28	0.1831
C5	0.1722	O13	-0.2688	C21	0.0152	O29	-0.2639
C6	-0.0815	O14	-0.1526	C22	0.0144	O30	-0.2848
H7	0.1466	O15	-0.3411	H23	0.1695	H31	0.2130
C8	-0.0301	O16	-0.3878	C24	-0.1771	H32	0.2202

Scheme 1

Scheme 1 is available in the Supplementary Files section.

Figures

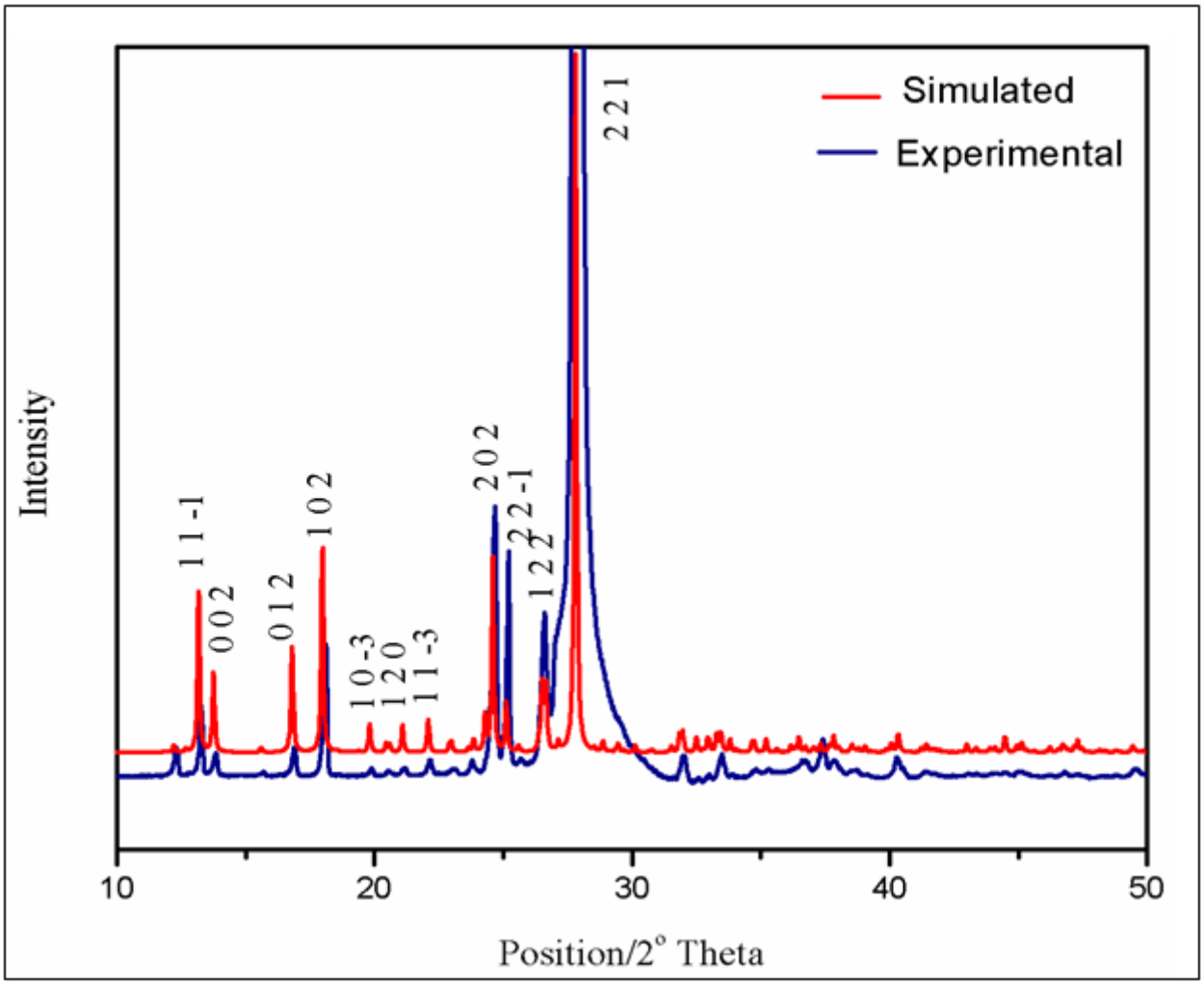

Figure 1

Simulated and experimental powder XRD patterns

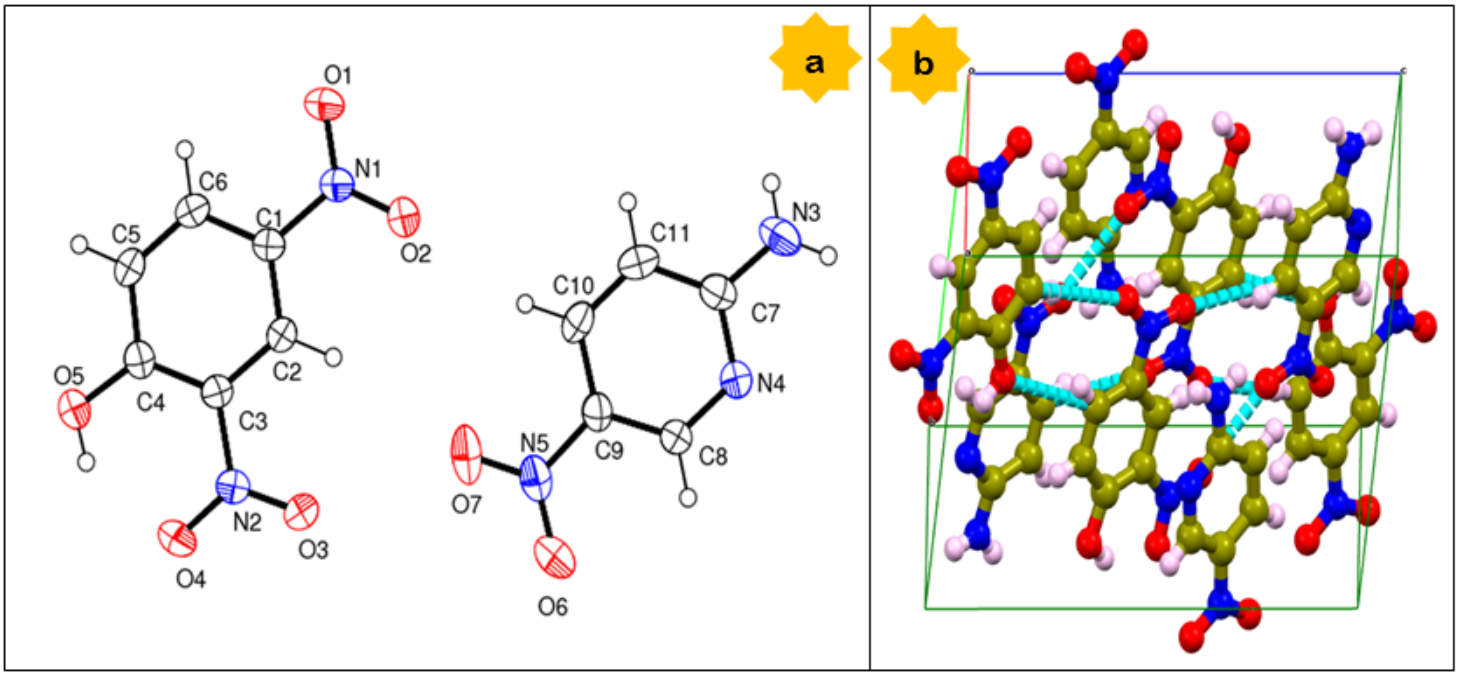

Figure 2

(a) ORTEP and (b) Molecular packing diagram of ANDP

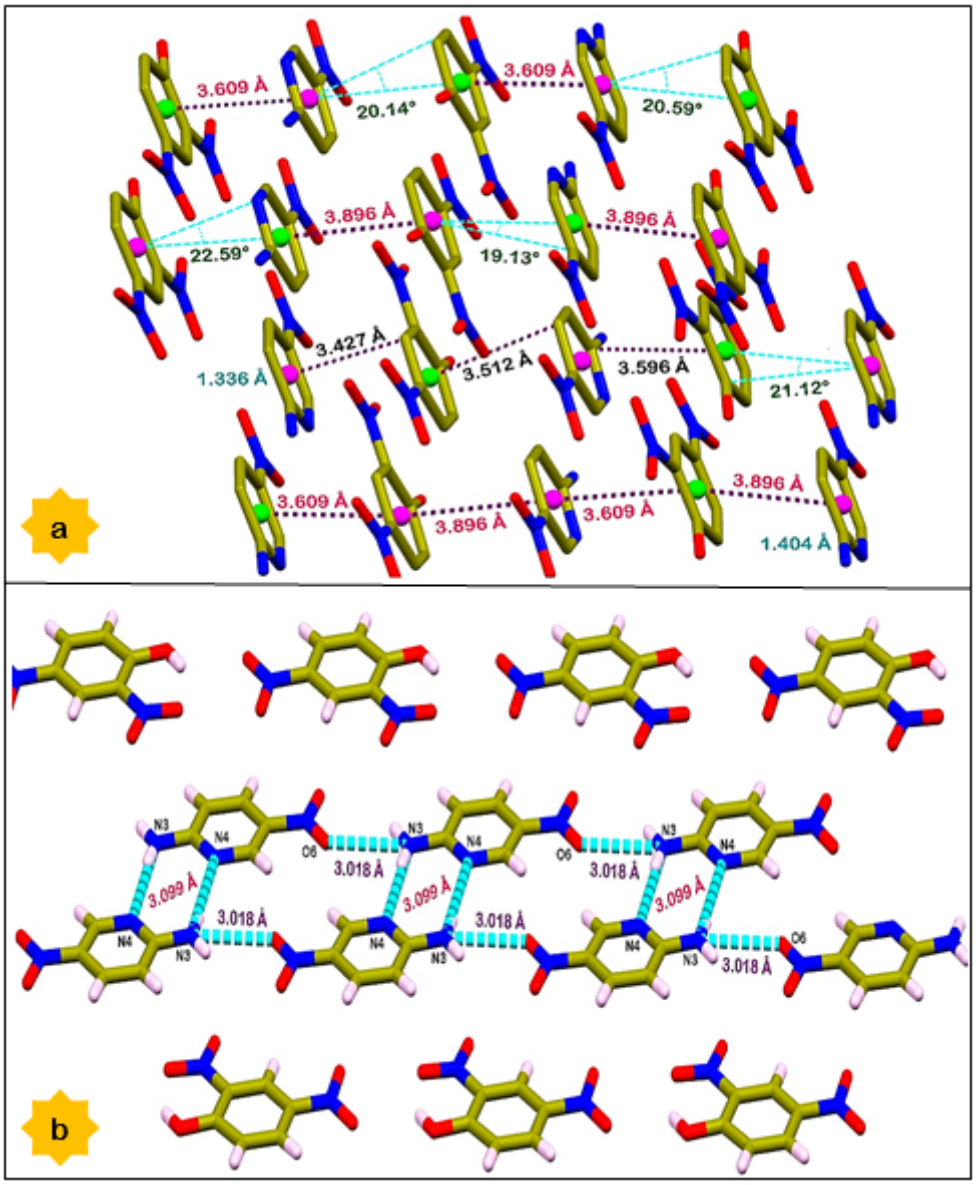

Figure 3

The structural details: (a) π•••π interactions (b) Molecular packing interactions of N- H•••O and N-H•••N

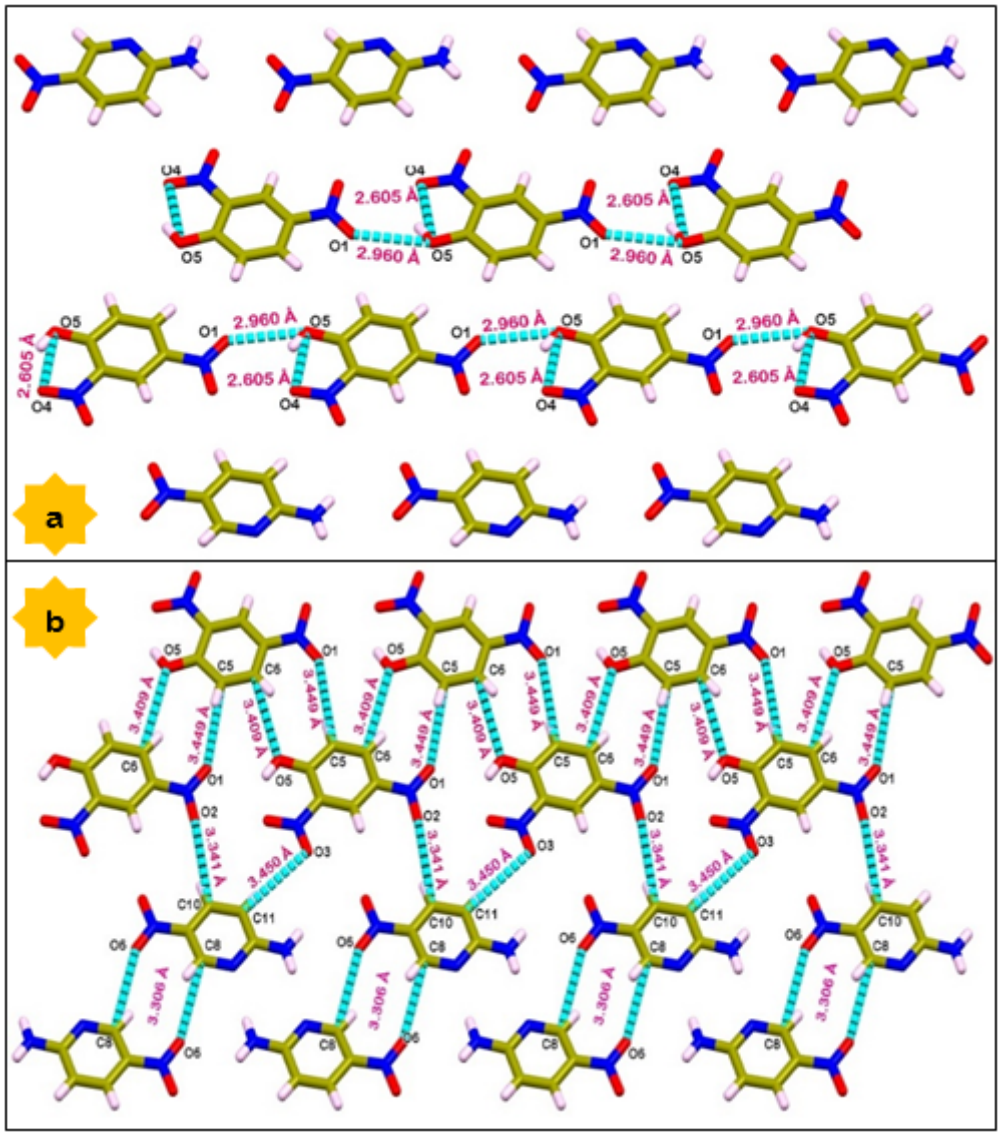

Figure 4

Molecular packing interactions along a-axis: (a) O-H•••O and (b) C-H•••O interactions of ANDP

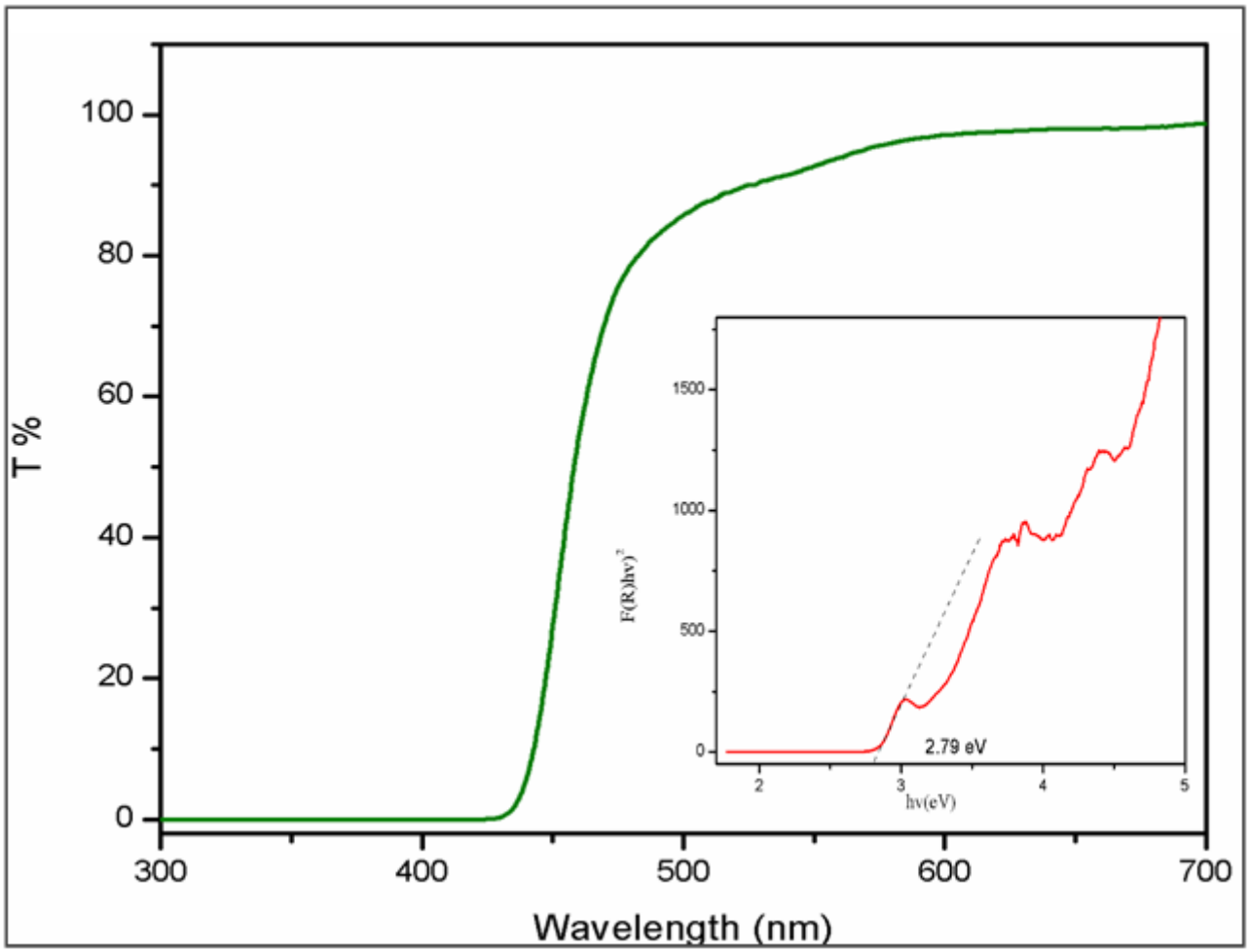

Figure 5

UV- Vis spectrum of ANDP (Tauc plot is given as an inset)

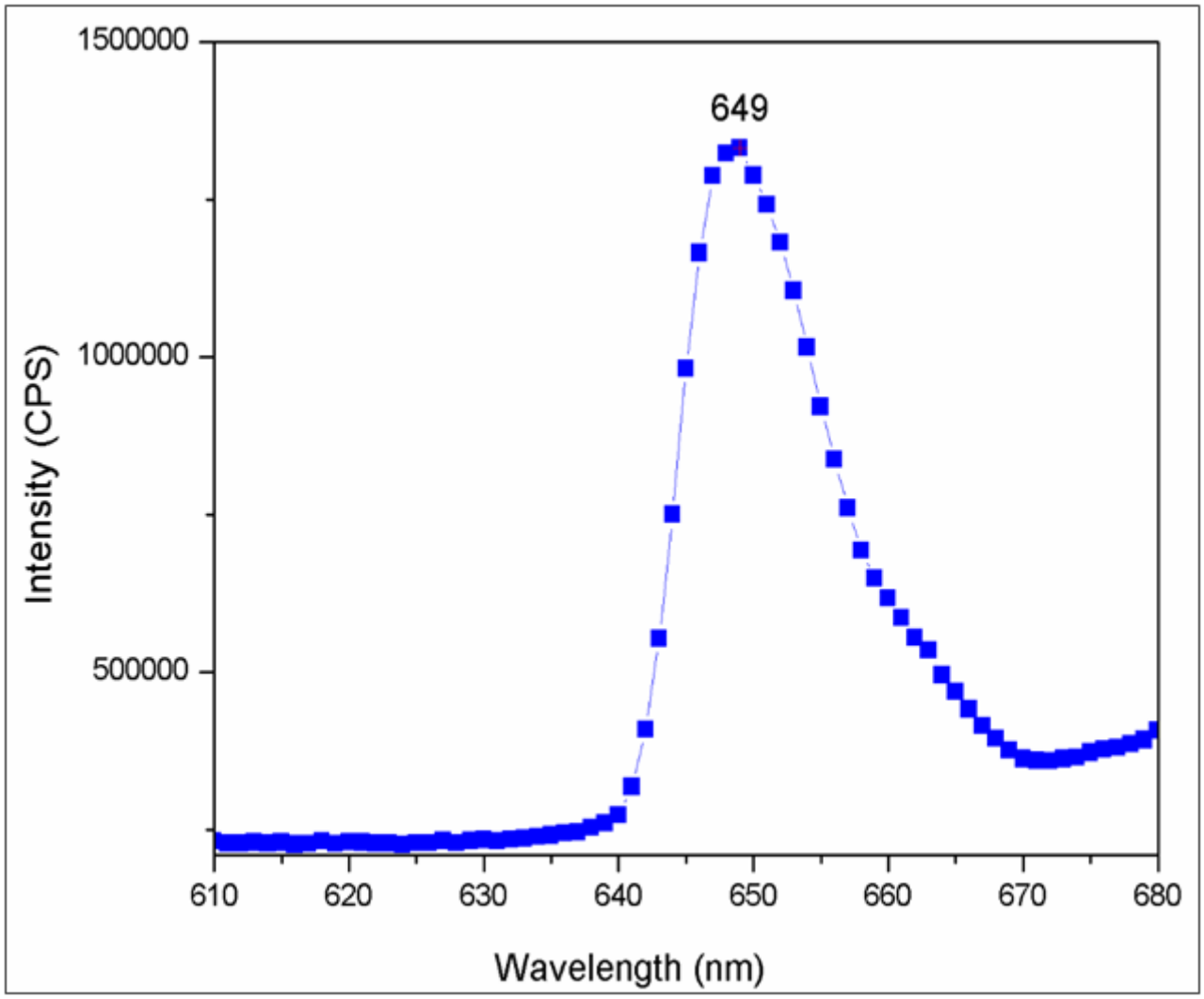

Figure 6

Photoluminescence spectrum of ANDP

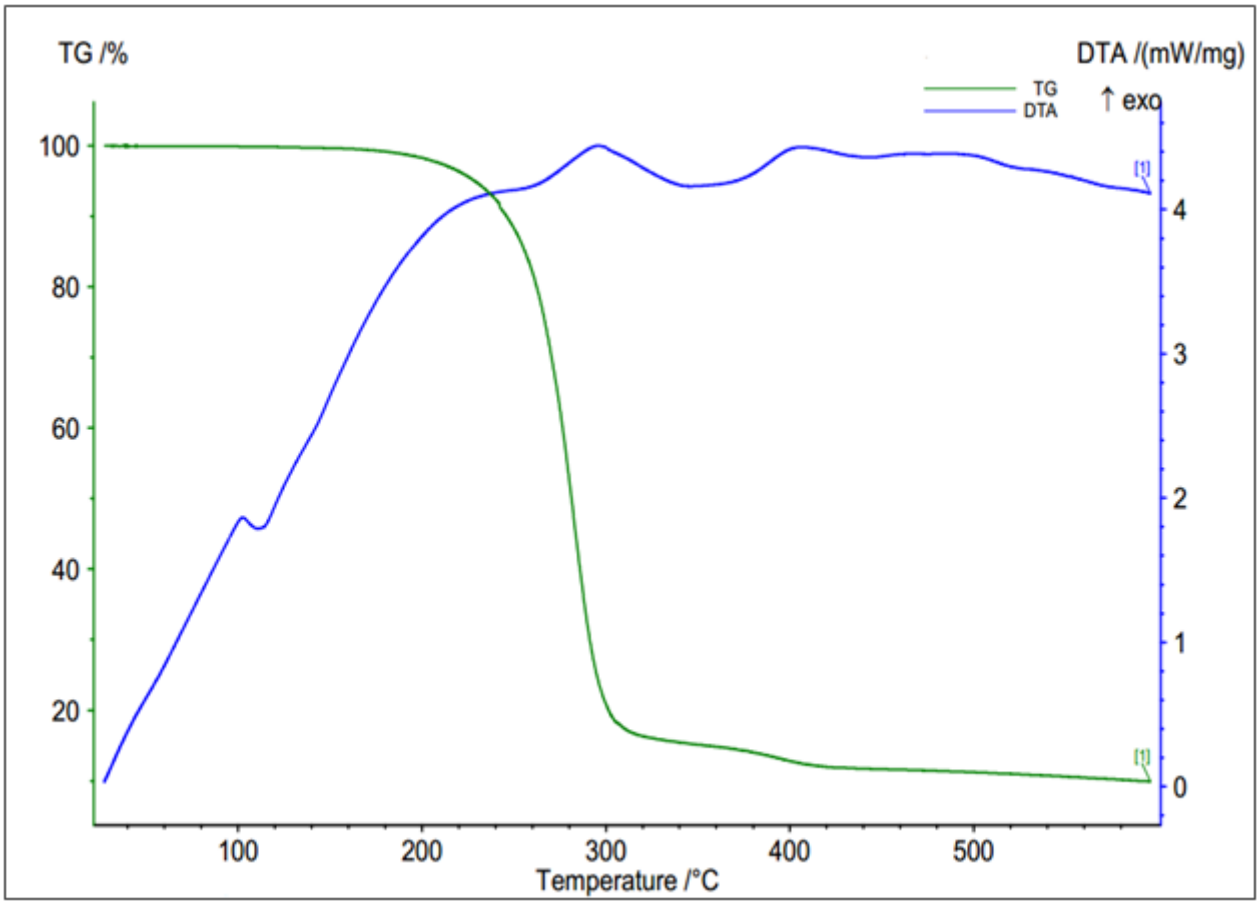

Figure 7

TG-DTA Curve of ANDP

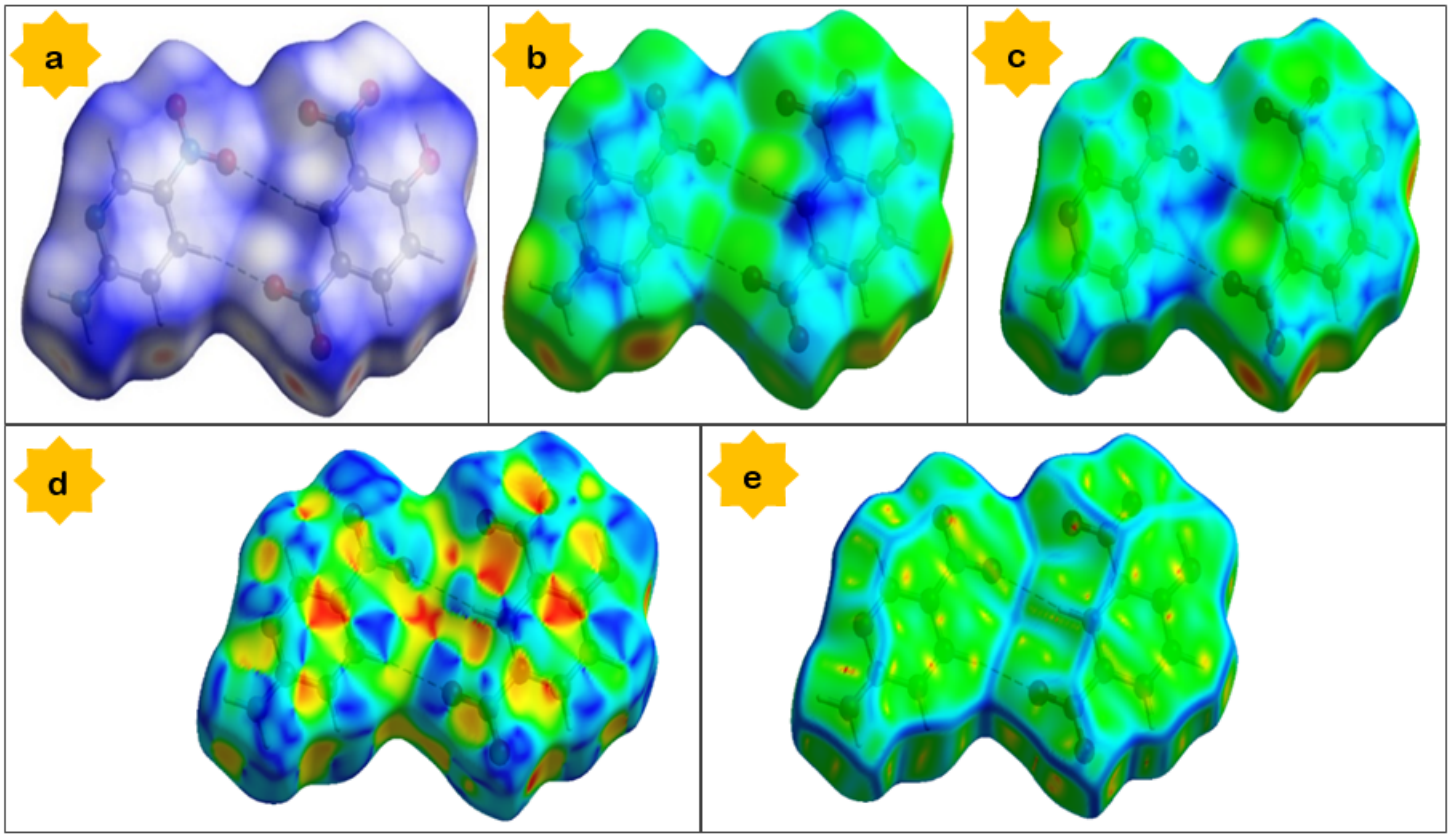

Figure 8

Hirshfeld surface (a) *d*norm (b) *di* (c) *de*(d) shape index and (e) curvedness

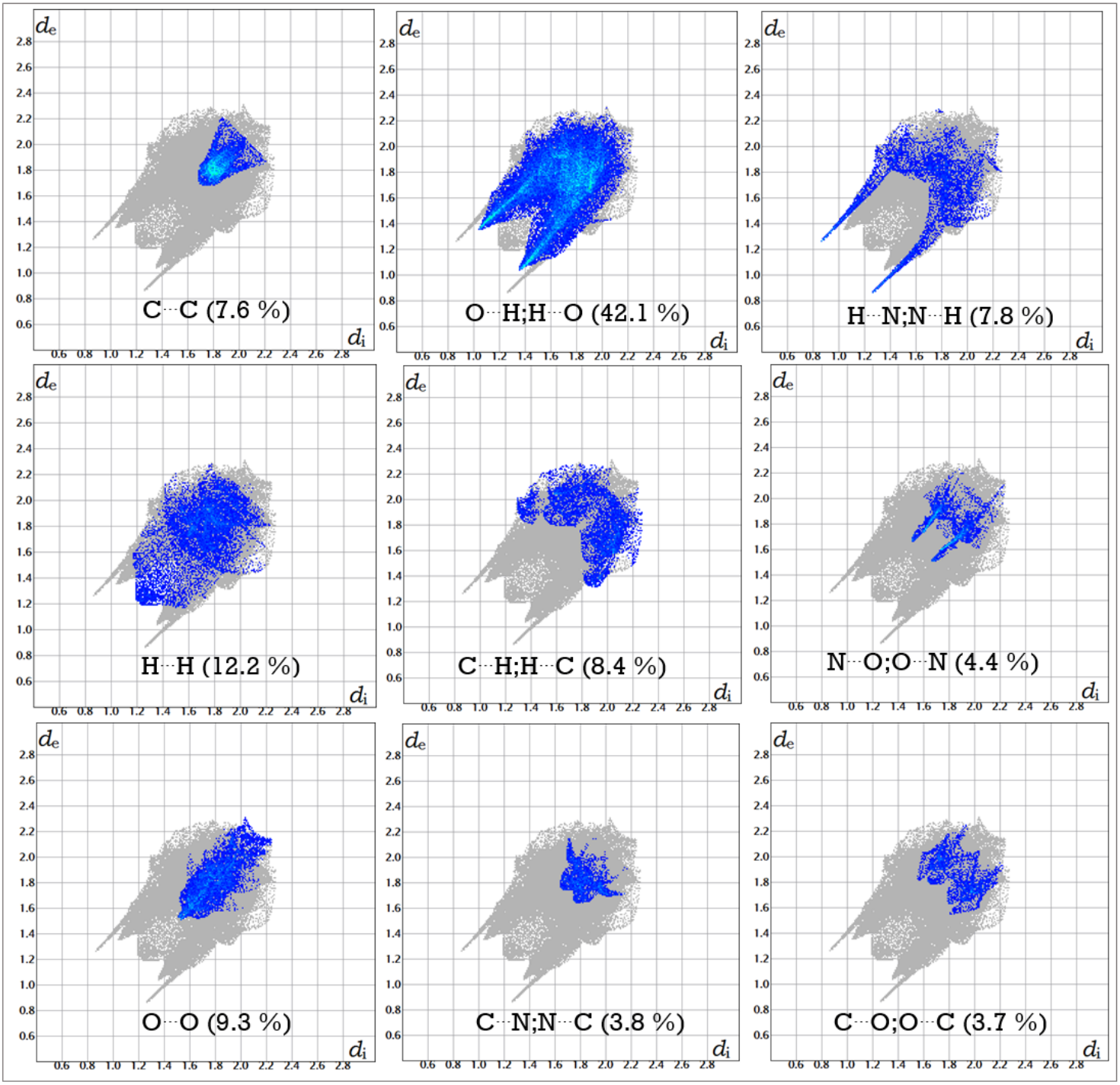

Figure 9

Fingerprint plots

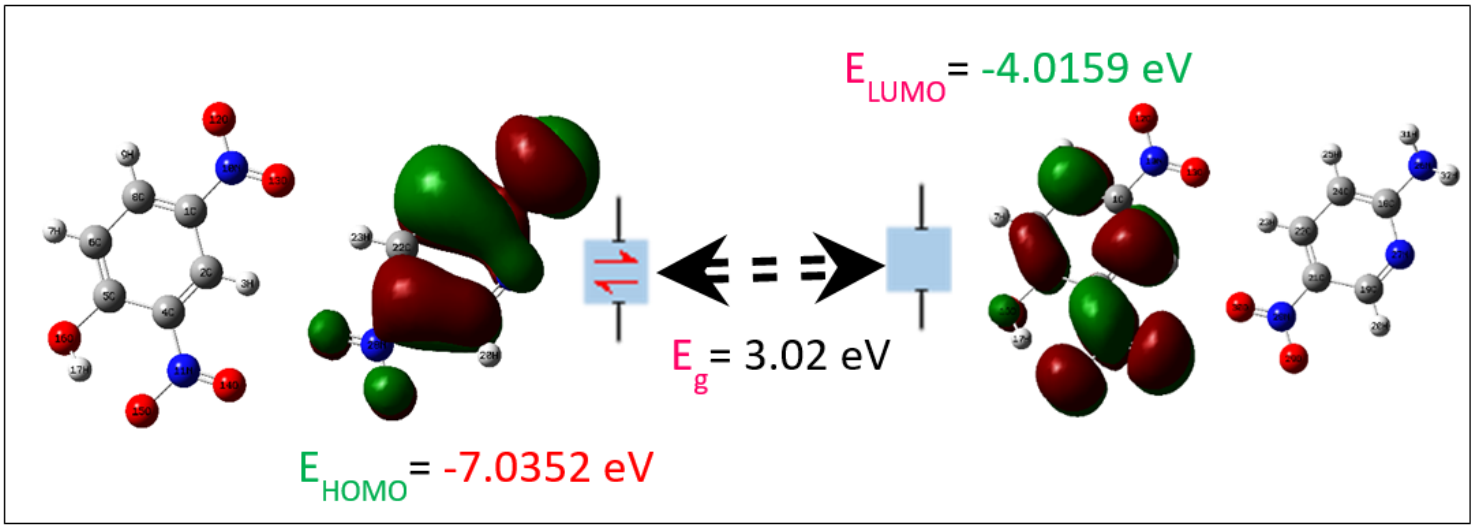

Figure 10

Frontier molecular orbital

Supplementary Files

This is a list of supplementary files associated with this preprint. Click to download.

- SupportingInformationFigures.docx
- SupportingInformationTables.docx
- Scheme1.png